Geophysical Research Letters

RESEARCH LETTER
10.1029/2022GL100594

Key Points:

- Optical, very high frequency, and low-frequency observations are combined to analyze the transition from upward to horizontal propagation of initial in-cloud lightning
- A drop in the optical blue-to-red ratio indicates when the dominant illumination process changes from streamers to likely stepped leader
- We find for in-cloud lightning that the upward initial leader and the horizontal stepped leader could be physically different

Correspondence to:
S. A. Cummer,
cummer@ee.duke.edu

Citation:
Huang, A., Cummer, S. A., Pu, Y., Chanrion, O. A., Neubert, T., Reglero, V., & Østgaard, N. (2022). Transition in optical and radio features during the early development of negative intracloud leader. *Geophysical Research Letters*, *49*, e2022GL100594. https://doi.org/10.1029/2022GL100594

Received 1 AUG 2022
Accepted 8 NOV 2022

Transition in Optical and Radio Features During the Early Development of Negative Intracloud Leader

Anjing Huang[1], Steven A. Cummer[1], Yunjiao Pu[1], Olivier A. Chanrion[2], Torsten Neubert[2], Victor Reglero[3], and Nikolai Østgaard[4]

[1]Electrical and Computer Engineering Department, Duke University, Durham, NC, USA, [2]National Space Institute, Technical University of Denmark (DTU Space), Kongens Lyngby, Denmark, [3]Image Processing Laboratory, University of Valencia, Valencia, Spain, [4]Birkeland Center for Space Science, University of Bergen, Bergen, Norway

Abstract What happens when the upward in-cloud (IC) breakdown transitions into horizontally expanding extension? Optical observations of this transition in IC lightning have not previously been reported. We identify the radio and optical signatures of this transition in low-frequency (LF) magnetic, very high frequency interferometric and space-borne optical measurements. For initial IC development in stratiform clouds, the ratio of 337/777.4 nm radiance is above unity prior to the transition but is almost always below unity after the transition. In particular, the 337 nm radiance drops significantly while the 777.4 nm radiance remains almost invariant after the transition, suggesting when the dominant illumination process of IC leaders changes from cold streamer discharges to a likely stepped leader. Furthermore, this transition in the LF and optical measurements resembles the reported changes in the cloud-to-ground measurements from initial leader to stepped leader, indicating that the initial leader may be physically different from the stepped leader.

Plain Language Summary The development of negative leaders within clouds remains intriguing and merits optical observation imperatively. Here, we report the optical observations of initial in-cloud (IC) leaders from a top view by a space-borne Atmosphere-Space Interactions Monitor on the International Space Station. After analyzing the dynamics of some upward IC flashes from very high frequency interferometry, we identify a clear transition in the initial development of IC leaders from upward propagation to sideways extension. We show that this transition also has repeatable signatures in the LF power density (1–300 kHz bandwidth) and optical waveforms. In our cases, the transition starts when the 337 (blue)/777.4 nm (red) brightness ratio drops significantly. The 337 nm radiance dominates the optical emissions prior to the transition but pronouncedly declines after the transition compared with the 777.4 nm radiance. The weakening of 337 nm radiance during the transition indicates a change in the dominant illumination processes of initial IC development. In addition, a similar variation identified from the observations of the initial IC and cloud-to-ground leaders suggests a connection between our transition and the reported transition from initial leader to stepped leader.

1. Introduction

What happens when an upward-propagating in-cloud (IC) lightning flash of limited horizontal extent transitions into bifurcated, sideways extensions has long been an open question (Coleman et al., 2003; Vonnegut, 1983). The upward to horizontal development of IC flashes, which is an important feature of bilevel IC flashes, has long been observed and analyzed by numerous interferometer and Lightning Mapping Array (LMA) observations (Marshall et al., 2013; Rison et al., 1999, 2016; Shao & Krehbiel, 1996; Stock et al., 2014; Thomas et al., 2001). Although Lyu et al. (2016) used low-frequency (LF) interferometry to find that the structure and stepped dynamics of initial IC leaders are distinct from highly branched initial cloud-to-ground (CG) leaders, only photographic observations of detailed initial CG development are available (e.g., Stolzenburg et al., 2014, 2016, 2019, 2020).

Rare optical observations of cloud-to-air flashes (Edens et al., 2014; Krehbiel et al., 2008; Stolzenburg et al., 2021) have discussed the highly intermittent features, the light-emitting patterns, and the escaping behaviors of cloud-to-air flashes. For IC flashes, luminosity measurements from ground-based photometric instruments have been presented (Stolzenburg et al., 2016, 2022; Wilkes et al., 2016). More optical observations of lightning in clouds are desired to detail the dynamical development of different physical processes in initial IC flashes.

Owing to the recent operations of space-borne equipment such as the Atmosphere-Space Interactions Monitor (ASIM) on the International Space Station, we have a chance to investigate the optical radiance of different IC lightning processes from a top view with less opacity of clouds compared to the ground-based observations. ASIM is equipped with photometers and cameras in selected bands, that is, 337.0 (blue) and 777.4 nm (red). The 777.4 nm radiation was found to correlate with current from fast developing and highly conducting hot leader channels while the 337 nm radiance was suggested to originate primarily in non-thermal discharges (i.e., streamers and coronas) (Montanyà et al., 2021). Specifically, streamers were suggested to appear in isolated corona discharges or occur at the front tip of hot channel leaders (Soler et al., 2020). Furthermore, two particular scenarios about the optical radiance of lightning were previously discussed. First, if a leader channel forms, the detected 337 nm radiation was suggested to be able to well depict the leader channels in the stratiform regions with low cloud tops (Montanyà et al., 2021). Second, many authors have reported electrical activities from the top of cloud due to streamers only (Dimitriadou et al., 2022; Edens, 2011; Husbjerg et al., 2022; Li et al., 2022; Liu et al., 2021; Soler et al., 2020, 2021). The negligible 777.4 nm optical radiance implies the absence of leader channel formation. In this study, we compare and analyze the simultaneous optical and radio signals from the initial IC development. We reconstruct the IC development by very high frequency (VHF) interferometry and find a clear transition in its early propagation. We find that this transition is also defined by repeatable (but different) features in the LF power density and optical waveforms. For flashes located in stratiform clouds, this transition starts when the ratio of 337/777.4 nm (blue/red) radiance drops below unity. For other cases located deeper inside opaque clouds, the optical ratio also notably declines through the transition. This common drop of the optical ratio accompanied by a distinct weakening of the corresponding LF power density after the transition indicates a physical change in the dominant illumination process. In addition, the remarkable resemblances between our transition and the transition from initial leader to stepped leader of CG flashes described in Stolzenburg et al. (2020) support the hypothesis that the initial leader may develop in the absence of continuously hot and highly conducting leader channels and may be physically different from the following stepped leader (Belz et al., 2020).

2. Data and Methods

We develop a method to automatically identify this transition in the initial IC development based on the VHF mapping results. It was reported that the subtle structures of lightning development can be imaged with our high bandwidth (>200 MHz) and fast time resolution (<0.5 μs) VHF interferometry (Huang et al., 2021; Pu & Cummer, 2019). We select 30 IC flashes from our interferometric observations in 2021 and manually identify this transition according to the changes in the fashions of initial IC propagation. Accordingly, we define three distinctly different propagation periods as Ascending Stage, Transition Stage, and Horizontal Stage.

Figure 1 illustrates our definition of these three stages. We choose a typical IC flash detected around Duke Forest (DU; 35.971°N and −79.094°E) at 09:00:34 UTC on 26 March 2021 as the example. As shown in Figures 1a and 1b, the propagation is dominated by sources confined largely to a narrow channel with successively upward motion in Ascending Stage. In Horizontal Stage, the leader is dominated by sources in multiple channels and exhibits dominantly horizontal propagation. The intermittent development of leader in the Horizontal Stage is consistent with previous LMA observations of IC flashes, which also showed that the initial IC breakdown branches in propagating through upper positive storm charge (e.g., Stock et al., 2014). Ascending Stage and Horizontal Stage are connected by the Transition Stage. In the Transition Stage, the upward slope of the interferometric mapping sources clearly decreases in elevation versus time. For these 30 VHF IC cases, the average time difference between the inception of flash and the start of transition is 2.09 ms.

Correspondingly, we compare the LF data from the Florida Institute of Technology (FT; 28.062°N and −80.624°E) with the interferometric results of those VHF-LF flashes. The bandwidth of LF sensors is approximately 1–300 kHz and the sampling frequency is 1 MHz. The FT LF sensor is 890.47 km away from the DU VHF interferometry system. This distance is similar to the average distance (typically in the range of 700–1,000 km) between the ASIM reported locations of flashes and our nearest LF sensors. Therefore, we consider the FT LF data as an effective agency to connect the interferometric results with ASIM detected flashes. As shown in Figure 1d, the transition starts when the LF power density reaches a maximum in the first large power peak crowds (6.7 ms) and the transition finishes when the average density and amplitude of LF power peaks noticeably decrease. Considering the signatures of the precise end of the transition are not well defined for all cases, we

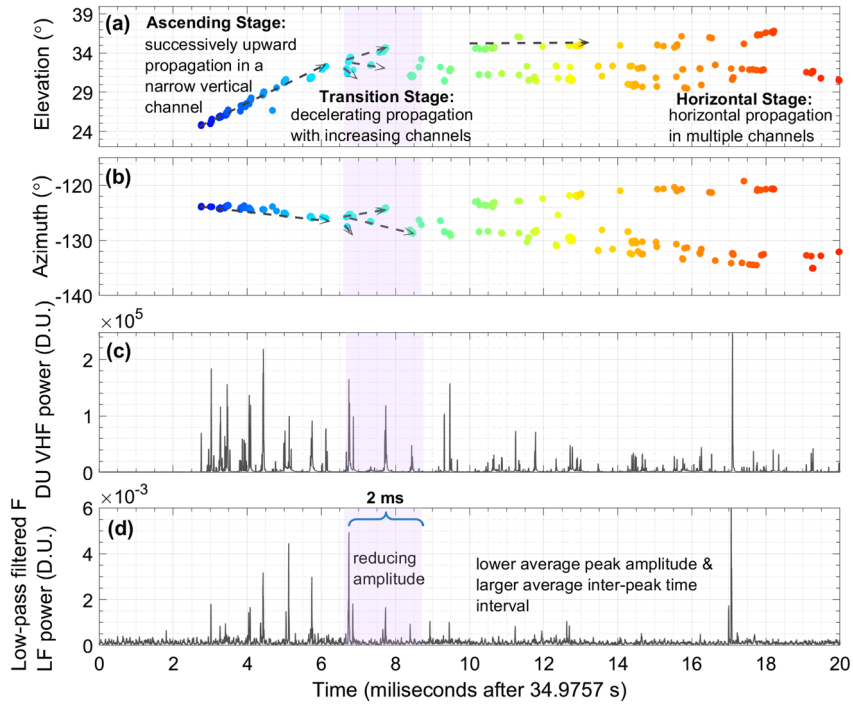

Figure 1. A typical in-cloud (IC) flash to illustrate our definition of the three stages of initial IC flash development. The purple rectangles mark the manually identified Transition Stage. Panels (a and b) are very high frequency (VHF) mapping results (in 100–200 MHz bandwidth) from Duke Forest (DU) plotted in elevation versus time and in azimuth versus time. Panels (c and d) are the power of DU VHF and Florida Institute of Technology low-frequency (LF) signals. The LF power in panel (d) is filtered by a band-pass with 30 and 300 kHz cut-off frequencies. For all the cases shown in this work, the propagation time of lightning radiation was subtracted.

arbitrarily define the duration of the Transition Stage as 2 ms, which captures the main features of the Transition Stage in our experience.

The LF power density signals were filtered out for the LF below 30 kHz as the best indicators of the Transition Stage (Figure 1c). The idea of applying a low-pass filter comes from the wavelet transform processing of LF data. We find that this low-pass filter successfully helps this method automatically identify the start of our transition in all of our cases. The success of this processing may result from the instantaneous features of initial IC propagation, whose developing patterns could be mostly influenced by higher frequency components in its LF radiation. The LF power density is first computed as the square of 1,024 × 14 samples (~14 ms) of the signals. Then the selected data are subtracted by their average value to eliminate the DC component and are averaged over 10 μs to emphasize the dominant frequency components and to present an easier auto-identified result.

From October 2020 to May 2021, ASIM totally captured the partial development of 1,619 flashes within 1,000 km of at least one of our four operating LF stations (DU; FT; PR, Arecibo, Puerto Rico, 18.370°N and −66.754°E; TU, Texas Tech University, 33.582°N and −101.881°E). Among these flashes, the early development of 56 flashes was recorded by ASIM. Thus, we matched the nearest LF data of these 56 flashes and then discarded flashes with weak optical signals (e.g., with the maximum amplitude of radiance is smaller than 5 $\mu W/m^2$) and CG flashes. Because we chose flashes with relatively strong and easily distinguishable peaks, the uncertainty of the ASIM absolute time accuracy ~25 ms (Heumesser et al., 2021) can be reduced to ~0.1 ms by identifying the same optical pulses detected by ASIM and ground-based LF measurements. At last, we obtained the well-captured early development of 30 LF-ASIM IC flashes. Those flashes are analyzed with single station LF (at range <1,000 km) and ASIM data of 337 and 777 nm photometers.

Wu et al. (2015) speculated that the initial leaders mainly propagate horizontally above certain altitude because they found the upward propagation speed will decrease with increasing initiation altitude. They also found an IC flash was horizontally initiated at 14.5 km. Their conclusions from observations are targeted at general situations without specifying convective or stratiform flashes. In addition, our stratiform LF-ASIM IC sferics show strong

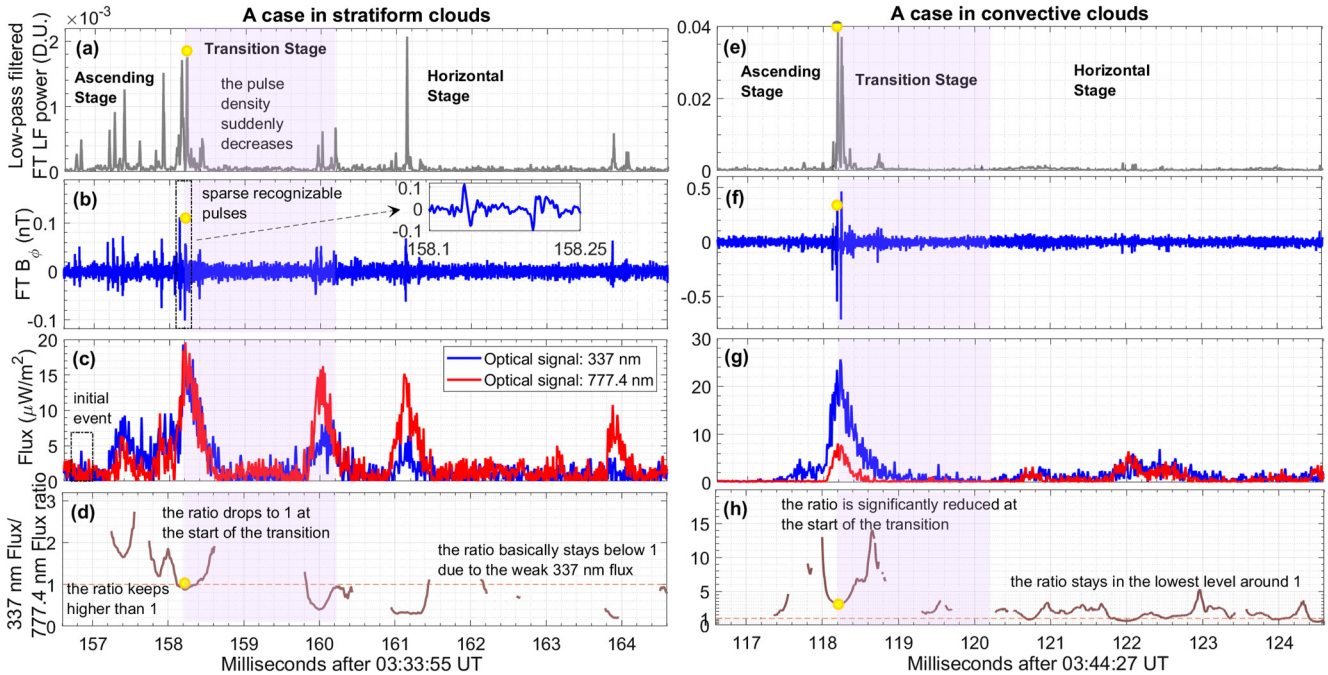

Figure 2. The comparison between optical emissions from Atmosphere-Space Interactions Monitor (ASIM) and low-frequency (LF) signals from the Florida Institute of Technology (FT) of two typical in-cloud flashes detected in stratiform clouds and in convective clouds. The purple rectangles mark the transition which was identified from LF signals based on the definition of the transition in Figure 1. The yellow highlighted circles mark the start time of the Transition Stage in different measurements. Panels (a and e) are the LF power densities computed from the same method as Figure 1d. Panels (b and f) are the $B\varphi$ components of the FT LF magnetic signals. The "classic" initial breakdown pulses are shown in the expanded view in panel (b). Panels (c and g) are the optical radiance from ASIM. Panels (d and h) are the ratios of 337/777.4 nm optical radiance. If either optical emission is at or below the background noise level, the optical ratio is not plotted to avoid meaningless ratios.

pulses before the transition and weak emissions after the transition. Those features are similar to sferics of our VHF-LF IC flashes whose VHF mapping results start with upward onset. But, we are unsure if our stratiform LF-ASIM cases were initiated vertically or not. Nonetheless, our transition focuses on the physical change from the streamer-dominated to the likely stepped leader phase, which applies whether the initial development is vertical or horizontal.

3. Results and Discussions

3.1. One Typical Case on 30 November 2020

Among these 30 LF-ASIM IC flashes, we first present the flash in Figure 2 at 03:33:55 UTC on 30 November 2020 to compare the LF and optical observations in detail. The early development of this flash was fortunately located in the stratiform region of a thundercloud according to the NEXRAD radar data from NOAA, the ASIM camera frames and NLDN records (Lang et al., 2004). Taking the early development region of this flash as the target region, we find the top of the target cloud is at height of 7.22 km above mean sea level, with a 15.5 dBZ averaged reflectivity, and a −21.3°C temperature from the radar data and the sounding data from University of Wyoming. The 15.5 dBZ averaged reflectivity of the target region is much lower than 30 dBZ, which is the threshold for the classification of stratiform and convective regions (Wetchayont et al., 2013). The reflectivity data are also uniformly distributed in the target region (with a maximum 5 dBZ difference). Therefore, the early development of this flash was in a relatively translucent stratiform region. Note that for our stratiform cases, the Transition Stage always begins when the optical ratio crosses unity. This consistency supports the conclusion that the propagation of the upward leader in the stratiform region can be well resolved by ASIM after we minimize the effects from cloud particles (Montanyà et al., 2021).

In Figure 2d, the ratio of 337/777.4 nm radiance stays greater than unity in Ascending Stage. Although being stronger than the 777.4 nm radiance, the variations of the 337 nm radiance are strongly correlated with the changes

in the 777.4 nm radiance. This suggests that the 337 nm emissions, which are dominantly produced from streamer discharges at channel tips, occur simultaneously with the formation of hot leader channels. It should be noted that laboratory measurements of long sparks have shown that the hot "unusual plasma features (UPFs)" can emit 337 nm-dominated radiation before large-scale hot conducting channels have formed (Kostinskiy et al., 2020). However, whether UPF-like processes known from laboratory measurements occur in natural lightning is still unknown, and we thus interpret the 337 nm emissions in the context of streamers rather than UPFs.

The transition of this stratiform flash starts around the time when the radiance in both bands reaches the maximum and the optical ratio declines to unity. Figure 2c shows that the blue radiance is much smaller after the transition while the red radiance remains almost invariant. Therefore, we suggest that the dominant illumination process for this case has a physical transition from cold corona discharges to excitation by a likely stepped leader (Soler et al., 2020, 2021).

In addition, the initial event of this flash appears at around 156.8 ms corresponding to only a subtle burst of the 337 nm radiance in Figure 2c with no distinguishable signal occurs in the 777.4 nm band, consistent with observations from the high-speed videos that only a little or no visible luminosity coincident with the initial events (Stolzenburg et al., 2021). Here, we further suggest the weak luminosity of this initial event could be created by streamers due to the absence of 777.4 nm radiance (Soler et al., 2020).

By comparing the LF waveforms in Figure 2b with the optical ratio in Figure 2d, we can find the blue/red optical ratio decreases when "classic" initial breakdown pulses ("classic" IBPs defined by pulse widths 10–80 us) occur and increases when no explicit impulsive peaks appear (Nag et al., 2009; Stolzenburg et al., 2020). The temporary decrease of the blue/red ratio accompanied by the concurrent "classic" IBPs may suggest that the power in the ambient *E*-field has been gradually transformed to enhance the formation of highly conducted leader channels through the IBPs. This interpretation can also be supported by the laboratory results which suggest that when two groups of "UPF networks" connect, a brief, large current will occur and produce classic IBPs in sferics (Kostinskiy et al., 2020). Those observations support conclusions from previous work of early CG development (e.g., Belz et al., 2020; Karunarathne et al., 2020; Stolzenburg et al., 2013, 2014, 2020) that "classic" IBPs successively change the non-conductive air into an ionized path for the following self-advancing stepped leader.

3.2. Overall Results for 30 ASIM-Detected IC Flashes

Common features of the stratiform cases can also be found in the convective case. As shown in Figures 2e–2h, this is a typical initial IC development detected at 03:44:27 UTC on 8 May. Although the blue/red optical ratio doesn't always drop to unity when the transition starts, the optical ratio for the case located in the deeper clouds greatly declines and is significantly reduced at the onset of the transition.

We also examine other well-captured flashes on a statistical basis to give a more general analysis of the transition process. Figure 3a shows that the average density and amplitude of the LF power peaks of LF-ASIM IC cases exhibit a pronounced decrease trend after the transition. Some cases also confirm that the red emissions are even temporarily intensified in Horizontal Stage while the blue emissions significantly decrease. The opposite behaviors of the dual-wavelength optical radiance indicate that optical change after the transition are not caused by changes in the intervening clouds. The blue histogram of LF-ASIM IC cases in Figure 3b justifies one phenomenon that we identify from the typical cases in Figure 2: the power density of the IBPs peaks around the time when both optical radiance reaches the maximum. The blue histogram shows that the time difference between maximum blue radiance and maximum LF power density is within 0.1 ms, suggesting the change in the LF power density is tightly associated with the variation of blue radiance in the early IC development. Therefore, we speculate that the transition may start when the charge densities at the vicinity of the newly formed, main leader channel reach the maximum. Strong corona discharges occur between the channel surface and ambient environment or occur at the tips of the newly formed leader. During the transition, plentiful charges on the leader could be rapidly depleted. In the following Horizontal Stage, the optical emissions from isolated streamer activities gradually reach the minimum, and the blue/red ratio drops to the lowest level while only few IBPs could be distinguished.

The red histogram of VHF-LF IC cases in Figure 3b shows that the average time difference of the start time of the transition identified from VHF maps and LF power density is within 0.1 ms, indicating that the repeatable features in the LF power density in different stages are reliable for defining the Transition Stage according to the VHF mapping results.

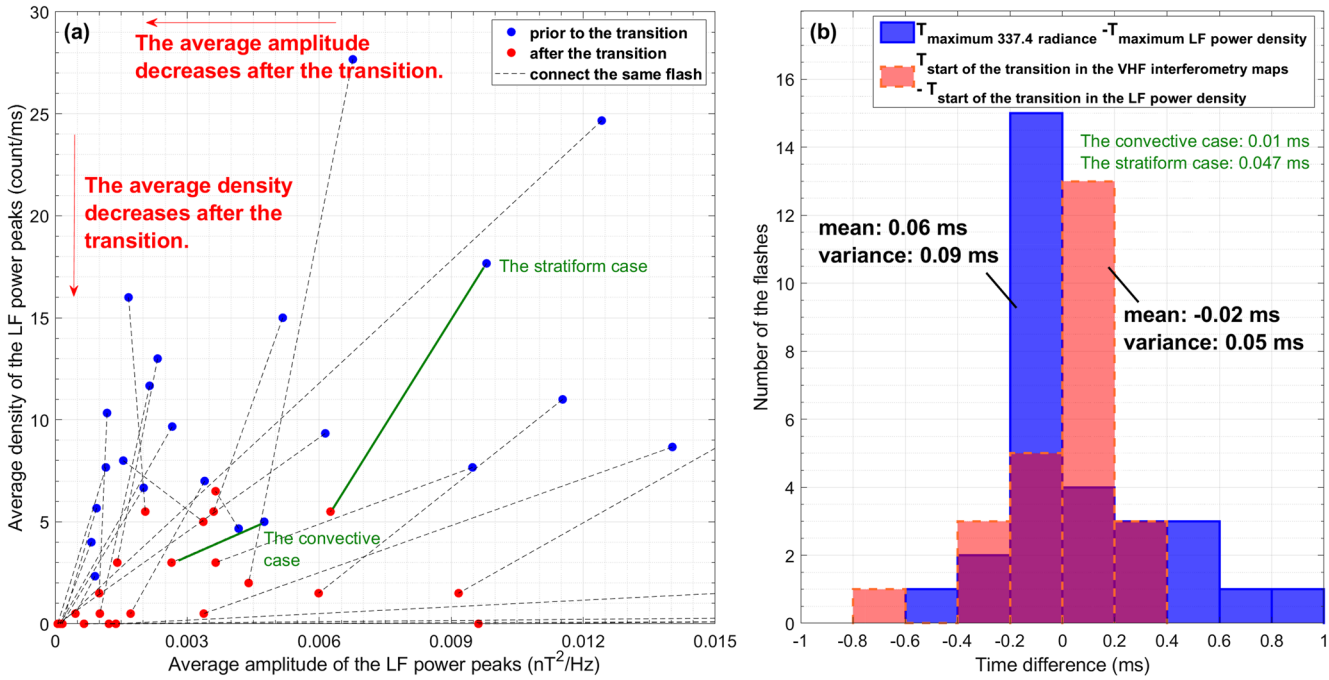

Figure 3. The statistics from all the very high frequency (VHF)-low-frequency (LF) and LF-Atmosphere-Space Interactions Monitor (ASIM) in-cloud (IC) flashes to present the common features of the transition. (a) The relationship between the average amplitude and the average density of the LF power peaks prior to and after the transition of 30 LF-ASIM IC cases. (b) Blue histogram: differences between the time of maximum 337 nm radiance and maximum LF power density of LF-ASIM IC cases. Red histogram: time differences between the start of the transition identified from VHF interferometric results and the corresponding LF power waveforms of VHF-LF IC cases. The corresponding values of cases in Figure 2 are marked with green texts and lines.

Additionally, remarkable similarities are found between our transition from upward propagation to horizontal extension and the transition from initial leader to stepped leader (Stolzenburg et al., 2020). Note that in the stratiform cases, the optical ratio will commonly cross unity when they exit the Ascending Stage. The unity value suggests the main, hot stepped leader is going to form through the transition due to almost equivalent and synchronized optical emissions from streamers and leader channels. Stolzenburg et al. (2020) proposed that the hot leader channel is fully formed after transitioning from initial leader and then the optical emissions of streamers in front of leaders should be accompanied by emissions originated from thermal excitation (Soler et al., 2020). Thus, it is highly probable that our transition is also the transition from initial leader to stepped leader as proposed by Stolzenburg et al. (2020) from high-speed observations of CG flashes. Moreover, they suggest the initial leader starts to bifurcate during or just after the largest IBP within 1 ms, coincident with the maximum brightness in videos, indicating that the largest IBP also may play a significant role in the transition from initial leader to stepped leader in CG flashes. Stolzenburg et al. (2020) also suggest the transition to stepped leader begins when the leader length remains dimly lit between burst, consistent with the lack of impulsive optical and LF peaks in our Transition Stage. The distinctively decreased LF peaks in the Horizontal Stage shown in Figure 3a also agree with the much smaller *E*-change pulses in the stepped leader stage of their CG observations. In summary, the high resemblances between the transitions observed in IC and CG lightning provide supports of the hypothesis that the initial leader and stepped leader may be physically different.

4. Conclusions

To better understand the initial IC development by optical observations from space-borne platforms, we develop a method to identify different developing stages of initial IC leaders by comparing LF magnetic field measurements with corresponding optical observations and VHF interferometry. According to the mapped IC leader development from VHF interferometry, a distinct transition in the initial IC development is defined from limited horizontal extent, upward propagation to horizontal extension with multiple branches. This transition can also be identified by specific features in the LF power density and optical waveforms. Accordingly, the initial IC development is divided into Ascending Stage, Transition Stage, and Horizontal Stage as summarized in Figure 4.

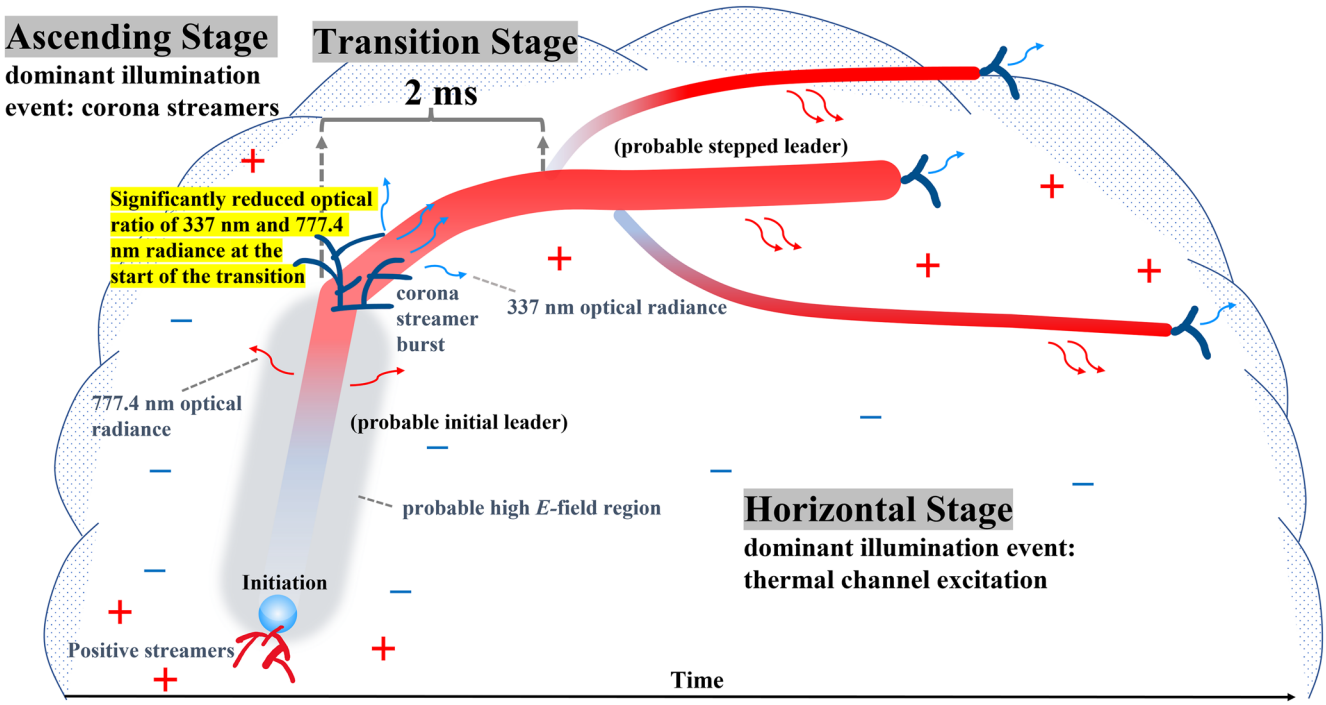

Figure 4. A summarized diagram of the early development of in-cloud (IC) flashes in three stages. The time duration of the Transition Stage is empirically defined as 2 ms. The IC leaders are plotted from blue to red, suggesting the channels are developing from dielectric condition to conductive condition. The background geometry behind the leaders plotted in gray indicates the possible high *E*-field region exists before Transition Stage.

Typical features of this transition are first identified according to cases located in stratiform clouds whose optical emissions are well resolved by ASIM (Montanyà et al., 2021). In Ascending Stage, the optical ratio of 337/777.4 nm radiance is generally greater than unity. The optical ratio declines to unity upon the start of the Transition Stage. In Horizontal Stage, the optical ratio drops below unity due to the significantly weakening blue radiance and nearly constant red radiance. For other cases located deeper in thunderclouds, the optical ratio is reduced upon the onset of the Transition Stage and declines to its lowest level in Horizontal Stage. In summary, we suggest the dominant illumination process changes from corona streamer activities to likely stepped leader through this transition and the features in the 337/777.4 nm radiance optical ratio tell when the transition starts. Furthermore, the sharp and common decrease of the average amplitude and density of LF power peaks after the transition suggests the possible departure from the high *E*-field region of the IC leader tip.

Finally, lack of impulsive optical and LF peaks in our Transition Stage and the distinctively decreased LF peaks in the Horizontal Stage suggest that our transition could also be the transition from initial leader to stepped leader identified in CG flashes by Stolzenburg et al. (2020). Marshall et al. (2013) also suggested that the initial leader stage in IC flashes ends when the gap between middle negative and upper positive charge layers was filled, supporting that the IC leader in our Horizontal Stage could be the stepped leader after the initial leader stage. Therefore, the well-regulated changes of the optical ratio and sferics through our transition may support their conclusions that the high conductivity, hot channel is not fully formed for initial leader and thus the initial leader is physically different from the stepped leader.

To the best of our knowledge, this work reports optical observations of the transition in the early development of negative leader in clouds for the first time. From this work, we suggest that multi-instrument measurements comparing observations from space-borne and ground-based instruments would be valuable. Nonetheless, this study provides more associations between different LF signatures and optical detections, which might help improve our current understanding of IC flashes.

Data Availability Statement

This work complies with the AGU data policy. The data plotted are available online (https://doi.org/10.5281/zenodo.6950838).

Acknowledgments
This study is supported by the National Science Foundation Dynamic and Physical Meteorology program through grant AGS-2026304. We would like to thank Dr. Fanchao Lyu for his contributions in establishing the interferometry system used here.

References

Belz, J. W., Krehbiel, P. R., Remington, J., Stanley, M. A., Abbasi, R. U., LeVon, R., et al. (2020). Observations of the origin of downward terrestrial gamma-ray flashes. *Journal of Geophysical Research: Atmospheres*, *125*(23), 1–26. https://doi.org/10.1029/2019JD031940

Coleman, L. M., Marshall, T. C., Stolzenburg, M., Hamlin, T., Krehbiel, P. R., Rison, W., & Thomas, R. J. (2003). Effects of charge and electrostatic potential on lightning propagation. *Journal of Geophysical Research*, *108*(9), 1–27. https://doi.org/10.1029/2002jd002718

Dimitriadou, K., Chanrion, O., Neubert, T., Protat, A., Louf, V., Heumesser, M., et al. (2022). Analysis of blue corona discharges at the top of tropical thunderstorm clouds in different phases of convection. *Geophysical Research Letters*, *49*(6), e2021GL095879. https://doi.org/10.1029/2021gl095879

Edens, H. E. (2011). Photographic and lightning mapping observations of a blue starter over a New Mexico thunderstorm. *Geophysical Research Letters*, *38*(17), L17804. https://doi.org/10.1029/2011GL048543

Edens, H. E., Eack, K. B., Rison, W., & Hunyady, S. J. (2014). Photographic observations of streamers and steps in a cloud-to-air negative leader. *Geophysical Research Letters*, *41*(4), 1336–1342. https://doi.org/10.1002/2013GL059180

Heumesser, M., Chanrion, O., Neubert, T., Christian, H. J., Dimitriadou, K., Gordillo-Vazquez, F. J., et al. (2021). Spectral observations of optical emissions associated with terrestrial gamma-ray flashes. *Geophysical Research Letters*, *48*(4), 1–10. https://doi.org/10.1029/2020GL090700

Huang, A., Cummer, S. A., & Pu, Y. (2021). Lightning initiation from fast negative breakdown is led by positive polarity dominated streamers. *Geophysical Research Letters*, *48*(8), e2020GL091553. https://doi.org/10.1029/2020GL091553

Husbjerg, L., Neubert, T., Chanrion, O., Dimitriadou, K., Li, D., Stendel, M., et al. (2022). Observations of blue corona discharges in thunderclouds. *Geophysical Research Letters*, *49*(12), e2022GL099064. https://doi.org/10.1029/2022gl099064

Karunarathne, N., Marshall, T. C., Karunarathne, S., & Stolzenburg, M. (2020). Studying sequences of initial breakdown pulses in cloud-to-ground lightning flashes. *Journal of Geophysical Research: Atmospheres*, *125*(3), 1–21. https://doi.org/10.1029/2019JD032104

Kostinskiy, A. Y., Marshall, T. C., & Stolzenburg, M. (2020). The mechanism of the origin and development of lightning from initiating event to initial breakdown pulses (v.2). *Journal of Geophysical Research: Atmospheres*, *125*(22), e2020JD033191. https://doi.org/10.1029/2020JD033191

Krehbiel, P. R., Riousset, J. A., Pasko, V. P., Thomas, R. J., Rison, W., Stanley, M. A., & Edens, H. E. (2008). Upward electrical discharges from thunderstorms. *Nature Geoscience*, *1*(4), 233–237. https://doi.org/10.1038/ngeo162

Lang, T. J., Rutledge, S. A., & Wiens, K. C. (2004). Origins of positive cloud-to-ground lightning flashes in the stratiform region of a mesoscale convective system. *Geophysical Research Letters*, *31*(10), L10105. https://doi.org/10.1029/2004GL019823

Li, D., Luque, A., Lehtinen, N. G., Gordillo-Vázquez, F. J., Neubert, T., Lu, G., et al. (2022). Multi-pulse corona discharges in thunderclouds observed in optical and radio bands. *Geophysical Research Letters*, *49*(13), e2022GL098938. https://doi.org/10.1029/2022GL098938

Liu, F., Lu, G., Neubert, T., Lei, J., Chanrion, O., Ostgaard, N., et al. (2021). Optical emissions associated with narrow bipolar events from thunderstorm clouds penetrating into the stratosphere. *Nature Communications*, *12*(1), 1–18. https://doi.org/10.1038/s41467-021-26914-4

Lyu, F., Cummer, S. A., Lu, G., Zhou, X., & Weinert, J. (2016). Imaging lightning intracloud initial stepped leaders by low-frequency interferometric lightning mapping array. *Geophysical Research Letters*, *43*(10), 5516–5523. https://doi.org/10.1002/2016GL069267

Marshall, T., Stolzenburg, M., Karunarathne, S., Cummer, S., Lu, G., Betz, H.-D., et al. (2013). Initial breakdown pulses in intracloud lightning flashes and their relation to terrestrial gamma ray flashes. *Journal of Geophysical Research: Atmospheres*, *118*(19), 10907–10925. https://doi.org/10.1002/jgrd.50866

Montanyà, J., López, J. A., Morales Rodriguez, C. A., van der Velde, O. A., Fabró, F., Pineda, N., et al. (2021). A simultaneous observation of lightning by ASIM, Colombia-lightning mapping array, GLM, and ISS-LIS. *Journal of Geophysical Research: Atmospheres*, *126*(6), 1–17. https://doi.org/10.1029/2020JD033735

Nag, A., DeCarlo, B. A., & Rakov, V. A. (2009). Analysis of microsecond- and submicrosecond-scale electric field pulses produced by cloud and ground lightning discharges. *Atmospheric Research*, *91*(2–4), 316–325. https://doi.org/10.1016/j.atmosres.2008.01.014

Pu, Y., & Cummer, S. A. (2019). Needles and lightning leader dynamics imaged with 100–200 MHz broadband VHF interferometry. *Geophysical Research Letters*, *46*(22), 2019GL085635. https://doi.org/10.1029/2019GL085635

Rison, W., Krehbiel, P. R., Stock, M. G., Edens, H. E., Shao, X. M., Thomas, R. J., et al. (2016). Observations of narrow bipolar events reveal how lightning is initiated in thunderstorms. *Nature Communications*, *7*, 1–12. https://doi.org/10.1038/ncomms10721

Rison, W., Thomas, R. J., Krehbiel, P. R., Hamlin, T., & Harlin, J. (1999). A GPS-based three-dimensional lightning mapping system: Initial observations in Central New Mexico. *Geophysical Research Letters*, *26*(23), 3573–3576. https://doi.org/10.1029/1999gl010856

Shao, X. M., & Krehbiel, P. R. (1996). The spatial and temporal development of intracloud lightning. *Journal of Geophysical Research*, *101*(D21), 26641–26668. https://doi.org/10.1029/96JD01803

Soler, S., Gordillo-Vazquez, F. J., Perez-Invernon, F. J., Luque, A., Li, D., Neubert, T., et al. (2021). Global frequency and geographical distribution of nighttime streamer corona discharges (BLUEs) in thunderclouds. *Geophysical Research Letters*, *48*(18), e2021GL094657. https://doi.org/10.1029/2021gl094657

Soler, S., Pérez-Invernón, F. J., Gordillo-Vázquez, F. J., Luque, A., Li, D., Malagón-Romero, A., et al. (2020). Blue optical observations of narrow bipolar events by ASIM suggest corona streamer activity in thunderstorms. *Journal of Geophysical Research: Atmospheres*, *125*(16), 1–13. https://doi.org/10.1029/2020JD032708

Stock, M. G., Akita, M., Krehbiel, P. R., Rison, W., Edens, H. E., Kawasaki, Z., & Stanley, M. A. (2014). Continuous broadband digital interferometry of lightning using a generalized cross-correlation algorithm. *Journal of Geophysical Research*, *119*(6), 3134–3165. https://doi.org/10.1002/2013JD020217

Stolzenburg, M., Marshall, T. C., Bandara, S., Hurley, B., & Siedlecki, R. (2021). Ultra-high speed video observations of intracloud lightning flash initiation. *Meteorology and Atmospheric Physics*, *133*(4), 1177–1202. https://doi.org/10.1007/s00703-021-00803-3

Stolzenburg, M., Marshall, T. C., Bandara, S., & Siedlecki, R. (2022). Luminosity with large amplitude pulses after the initial breakdown stage in intracloud lightning flashes. *Atmospheric Research*, *267*, 105982. https://doi.org/10.1016/j.atmosres.2021.105982

Stolzenburg, M., Marshall, T. C., & Karunarathne, S. (2019). Inception of subsequent stepped leaders in lightning. *Meteorology and Atmospheric Physics*, *132*(4), 1–26. https://doi.org/10.1007/s00703-019-00702-8

Stolzenburg, M., Marshall, T. C., & Karunarathne, S. (2020). On the transition from initial leader to stepped leader in negative cloud-to-ground lightning. *Journal of Geophysical Research: Atmospheres*, *125*(4), 1–18. https://doi.org/10.1029/2019jd031765

Stolzenburg, M., Marshall, T. C., Karunarathne, S., Karunarathna, N., & Orville, R. E. (2014). Leader observations during the initial breakdown stage of a lightning flash. *Journal of Geophysical Research*, *119*(21), 12198–12221. https://doi.org/10.1002/2014JD02199

Stolzenburg, M., Marshall, T. C., Karunarathne, S., Karunarathna, N., Vickers, L. E., Warner, T. A., et al. (2013). Luminosity of initial breakdown in lightning. *Journal of Geophysical Research: Atmospheres*, *118*(7), 2918–2937. https://doi.org/10.1002/jgrd.50276

Stolzenburg, M., Marshall, T. C., Karunarathne, S., & Orville, R. E. (2016). Luminosity with intracloud-type lightning initial breakdown pulses and terrestrial gamma-ray flash candidates. *Journal of Geophysical Research: Atmospheres*, *121*(18), 10919–10936. https://doi.org/10.1002/2016JD025202

Thomas, R., Krehbiel, P., Rison, W., Hamlin, T., Harlin, J., & Shown, D. (2001). Observations of source powers radiated by lightning discharges. *Journal of Geophysical Research*, *28*(1), 143–146. https://doi.org/10.1029/2000gl011464

Vonnegut, B. (1983). Deductions concerning accumulations of electrified particles in thunderclouds based on electric field changes associated with lightning. *Journal of Geophysical Research*, *88*(C6), 3911–3912. https://doi.org/10.1029/JC088iC06p03911

Wetchayont, P., Hayasaka, T., & Katagiri, S. (2013). Application of a precipitating cloud classification method to radar observations in Thailand. *AIP Conference Proceedings*, *1531*, 388. https://doi.org/10.1063/1.4804788

Wilkes, R. A., Uman, M. A., Pilkey, J. T., & Jordan, D. M. (2016). Luminosity in the initial breakdown stage of cloud-to-ground and intracloud lightning. *Journal of Geophysical Research: Atmospheres*, *121*(3), 1236–1247. https://doi.org/10.1002/2015JD024137

Wu, T., Yoshida, S., Akiyama, Y., Stock, M., Ushio, T., & Kawasaki, Z. (2015). Preliminary breakdown of intracloud lightning: Initiation altitude, propagation speed, pulse train characteristics, and step length estimation. *Journal of Geophysical Research: Atmospheres*, *120*(18), 9071–9086. https://doi.org/10.1002/2015JD023546